

52 GHz 35% Scandium Doped Aluminum Nitride Overmoded Bulk Acoustic Resonator

Juhun Baek

Carnegie Mellon University
Pittsburgh, USA
juhunb@andrew.cmu.edu

Stephan Barth

Fraunhofer FEP
Dresden, Germany
stephan.barth@fep.fraunhofer.de

Tom Schreiber

Fraunhofer FEP
Dresden, Germany
tom.schreiber@fep.fraunhofer.de

Hagen Bartzsch

Fraunhofer FEP
Dresden, Germany
hagen.bartzsch@fep.fraunhofer.de

Gianluca Piazza

Carnegie Mellon University
Pittsburgh, USA
piazza@ece.cmu.edu

Abstract—Scandium doped Aluminum Nitride (ScAlN) has become a piezoelectric material of interest for Bulk Acoustic Wave (BAW) resonators as it offers an intrinsically high electromechanical coupling (k_t^2). However, little is known about ScAlN at mm-wave frequencies. In this work, we demonstrate an innovative Overmoded Bulk Acoustic Resonator (OBAR) design that incorporates 35% Scandium doped Aluminum Nitride (Sc_{0.35}Al_{0.65}N) piezoelectric layer. The ScAlN OBAR presented herein is a BAW device that is excited in the 2nd overtone by means of the ScAlN layer and a stack of metal electrodes that act simultaneously as acoustic cavity and as acoustic Bragg mirrors. The fabricated device demonstrates k_t^2 of 6.1% and Quality factor (Q) of 114 at 52 GHz – a substantial improvement in the $k_t^2 \cdot Q$ figure of merit of ScAlN acoustic resonators at mm-wave frequencies.

Index Terms—Scandium Aluminum Nitride (ScAlN), mm-wave resonator, acoustic resonator, overmoded bulk acoustic resonator (OBAR)

I. INTRODUCTION

Bulk Acoustic Wave (BAW) resonators are prevalent in the commercial market for signal filtering and timing applications below 6 GHz as they offer compact footprint and high performance [1]. As the industry continues the trend of moving towards higher frequency bands for faster wireless communications, the demand for compact high performance filters continues to increase.

However, significant challenges in scaling BAW resonators to operate at mm-wave frequencies still remain. Directly thinning down the piezoelectric layer thickness to increase resonant frequency results in thinner electrodes and reduced film quality, translating into a degradation in the electromechanical coupling (k_t^2) and quality factor (Q). Utilizing an overtone instead of the fundamental frequency to increase resonant frequency results in a severe reduction in k_t^2 due to charge cancellation in the piezoelectric material [2], [3]. Because the resonator k_t^2 and Q directly correlate to filter performance, such as bandwidth, insertion loss, out of band rejection and roll off [4], it is critical to address these challenges.

One method used to tackle these challenges has been research into novel resonator designs. The combined overtone

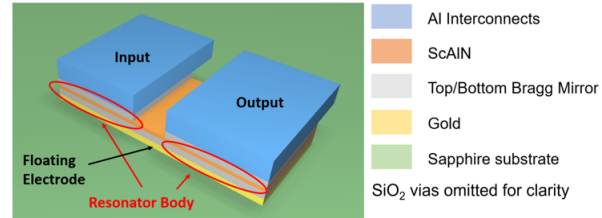


Fig. 1. 3D schematic of a unit ScAlN OBAR device. Multiple such units may be chained together.

resonators hybridize thickness and lateral extensional modes, enhancing the k_t^2 [5]. The periodically polarized resonators mitigate the effects of charge cancellation by inducing overtones through piezoelectric layers of alternating polarity [6], [7]. The solidly mounted Overmoded Bulk Acoustic Resonators (OBAR) use a second overtone to operate at mm-wave frequencies and incorporate partial transduction main cavity and acoustic Bragg mirrors to mitigate the k_t^2 degradation from operating in overtones [8], [9]. Fig. 1 shows a 3D schematic of a solidly mounted OBAR.

Another method used to tackle the challenges has been research and development of novel piezoelectric materials. Scandium doped Aluminum Nitride (ScAlN) has recently become a material of interest for BAW resonators as it has an intrinsically higher k_t^2 than Aluminum Nitride (AlN), and its material properties can be tuned by varying the amount of Scandium doping [10]. Additionally, ScAlN sputtering allows broad material choices for metal electrodes. In this work, we demonstrate the 35% ScAlN OBAR, combining the advantages of the ScAlN and the solidly mounted OBAR. The fabricated and measured ScAlN OBAR operates at 52 GHz, with k_t^2 of 6.1% and Q at series resonance of 114.

II. DESIGN AND FABRICATION

A. OBAR Design

The solidly mounted OBAR is comprised of the main cavity, the acoustic Bragg mirrors, and the electrodes. The main cavity

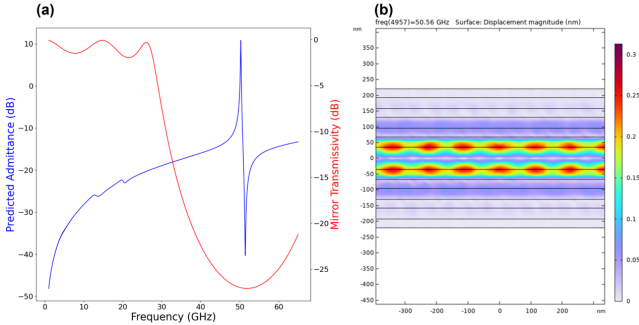


Fig. 2. (a) Mirror Transmissivity simulated with Mason equivalent circuit. (b) 2D FEA simulation of mechanical displacement for the ScAlN OBAR.

excites a second overtone through partial transduction, and confining as much acoustic energy as possible in this region is necessary to achieve high k_t^2 . The acoustic Bragg mirrors are alternating layers of materials with high and low acoustic impedance which reflect acoustic energy back into the main cavity. The electrodes route and connect the resonators. We model the acoustic Bragg mirror with the Mason equivalent circuit for thickness mode transducers [11] to simulate its transmissivity of acoustic energy. We optimize the Bragg mirror to best suppress undesired resonance modes while reflecting as much acoustic energy back into the ScAlN layer as possible around the resonant frequency. After establishing the Bragg mirror design, we use the Mason equivalent circuit simulations to optimize the ScAlN thickness to achieve resonant frequency of 50 GHz and highest k_t^2 possible. Then, we simulate the completed OBAR design with Finite Element Analysis (FEA) methods to verify the design. Fig. 1 shows the 3D schematic of ScAlN OBAR unit device, and Fig. 4 shows the finalized design cross section.

B. Device Fabrication

The fabrication flow for ScAlN OBAR is shown in Fig. 3. The process starts with the sputtering of metals and the 35% ScAlN ($\text{Sc}_{0.35}\text{Al}_{0.65}\text{N}$) onto a Sapphire substrate. These deposition steps are performed at Fraunhofer FEP [12]. The metal layers sandwich the ScAlN. The layers close to the ScAlN will form the acoustic Bragg mirror, while the layers furthest away will form the electrodes.

First, the top Bragg mirror is patterned with photoresist and ion milled until the ScAlN layer is reached. This patterns the top electrode of series connected resonators.

Second, the bottom Bragg mirror is patterned with photoresist and ion milled until the Sapphire substrate is reached. This defines a unit device formed by the series connection of 2 resonators through the floating electrode.

Third, a $1.1\ \mu\text{m}$ thick SiO_2 film is sputtered to form dielectric spacers for the routing electrodes between the resonators.

Fourth, the SiO_2 is patterned with photoresist and etched with an advanced oxide etcher. This anisotropic etch opens up the via holes for contacting the top electrodes.

Fifth, a $1.4\ \mu\text{m}$ thick aluminum film is sputtered, patterned with photoresist, and etched with a chlorine based reactive ion

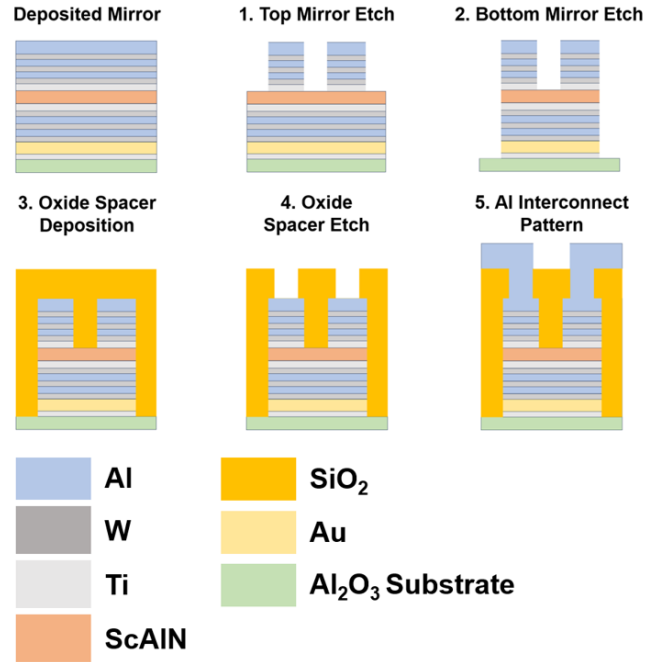


Fig. 3. Cross sectional diagram of ScAlN OBAR fabrication steps. The aspect ratio of the diagram is not to scale, and the lateral dimensions are approximately 100x larger than thickness dimensions.

etch. This forms the interconnects and the probe pads, finishing the fabrication process. The resulting device is encapsulated in an oxide matrix, with only the aluminum electrodes exposed to the environment. A thin coating of alumina can be deposited over the electrodes to hermetically seal the device if required.

III. MEASUREMENTS AND RESULTS

Fig. 4 shows a top down view of a fabricated ScAlN OBAR and its corresponding cross section. We measure the completed ScAlN OBARs on a Keysight PNA-X Microwave Network Analyzer with two $100\ \mu\text{m}$ pitch GSG probes. The overall setup is able to perform measurements up to a frequency of 67 GHz. We perform the calibration with a two-port short-open-load-thru (SOLT) reference standards on a calibration substrate.

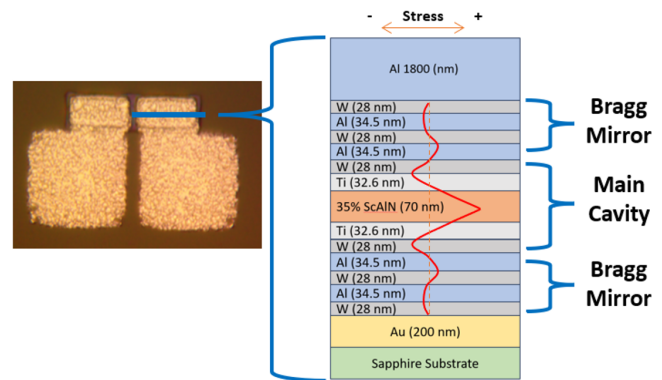


Fig. 4. Fabricated ScAlN OBAR and cross sectional diagram.

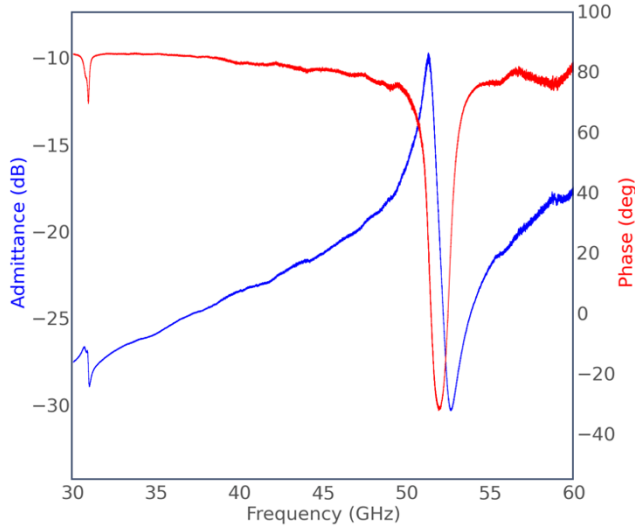


Fig. 5. Measured characteristic response of the ScAlN OBAR. Admittance (dB) is plotted with a blue trace, and the phase of admittance (°) is plotted with a red trace.

TABLE I
COMPARISON OF FIGURE OF MERITS BETWEEN SCALN OBAR SIMULATION AND MEASUREMENT

Figure of Merit	Design	Measured
f_s	50.3 GHz	51.3 GHz
f_p	51.6 GHz	52.6 GHz
k_t^2	6.2%	6.1%
Q_s	—	114
Q_p	—	67

We then perform de-embedding with the corresponding on-chip open and thru test structures and extract the admittance of the device under test. The measured admittance response is shown in Fig. 5.

The series resonant frequency (f_s) is 51.3 GHz, and the parallel resonant frequency (f_p) is 52.6 GHz. k_t^2 is extracted from the resonant frequencies [1], and is equivalent to:

$$k_t^2 = \frac{\pi}{2} \frac{f_s}{f_p} \tan\left(\frac{\pi(f_p - f_s)}{2f_p}\right) \quad (1)$$

To extract parameters such as Q at series resonance (Q_s) and Q at parallel resonance (Q_p), the measured admittance is fit to a modified Butterworth-Van Dyke (mBVD) model [13]. The extracted parameters and the comparison between design and the measurement are summarized in Table I. Compared to the simulated design, both the series and parallel resonant frequencies are 1 GHz higher. The measured k_t^2 of 6.1% is closely matched with the simulated k_t^2 of 6.2%. The measured Q_s of 114 is greater than measured Q_p of 67.

IV. CONCLUSION

In this work, we designed and fabricated a 35% ScAlN OBAR operating at 51.3 GHz. The demonstration achieves Q of 114 and k_t^2 of 6.1%, which is a significant improvement in figure of merit ($k_t^2 \cdot Q$) over the state of art mm-wave

ScAlN resonators [7], [14]. The ScAlN sputtering allows broad material choices for metal electrodes and facilitates incorporation of a fully encapsulated Bragg mirror used in solidly mounted OBAR. These characteristics show the ScAlN OBAR is a promising technology for mm-wave acoustics and filtering applications. Further studies into sources of loss, incorporation of periodically polarized ScAlN, and further screening of conductive materials for the Bragg mirror and electrodes will improve the ScAlN OBAR performance and provide significant advancements in mm-wave acoustics and its applications.

REFERENCES

- [1] R. Ruby, “11e-2 review and comparison of bulk acoustic wave fbar, smr technology,” in *2007 IEEE Ultrasonics Symposium Proceedings*, 2007, pp. 1029–1040.
- [2] A. Hagelauer, R. Ruby, S. Inoue, V. Plessky, K.-Y. Hashimoto, R. Nakagawa, J. Verdu, P. d. Paco, A. Mortazawi, G. Piazza, Z. Schaffer, E. T.-T. Yen, T. Forster, and A. Tag, “From microwave acoustic filters to millimeter-wave operation and new applications,” *IEEE Journal of Microwaves*, vol. 3, no. 1, pp. 484–508, 2023.
- [3] Y. Yang, R. Lu, L. Gao, and S. Gong, “10–60-ghz electromechanical resonators using thin-film lithium niobate,” *IEEE Transactions on Microwave Theory and Techniques*, vol. 68, no. 12, pp. 5211–5220, 2020.
- [4] S. Gong, R. Lu, Y. Yang, L. Gao, and A. Hassani, “Microwave acoustic devices: Recent advances and outlook,” *IEEE Journal of Microwaves*, vol. 1, pp. 601–609, 04 2021.
- [5] G. Giribaldi, L. Colombo, P. Simeoni, and M. Rinaldi, “Compact and wideband nanoacoustic pass-band filters for future 5g and 6g cellular radios,” *nature communications*, vol. 15, no. 1, p. 304, 2024.
- [6] J. Kramer, V. Chulukhadze, K. Huynh, O. Barrera, M. Liao, S. Cho, L. Matto, M. S. Goorsky, and R. Lu, “Thin-film lithium niobate acoustic resonator with high q of 237 and k2 of 5.1
- [7] W. Peng, S. Nam, D. Wang, Z. Mi, and A. Mortazawi, “A 56 ghz trilayer aln/scaln/aln periodically poled fbar,” in *2024 IEEE/MTT-S International Microwave Symposium - IMS 2024*, 2024, pp. 150–153.
- [8] Z. Schaffer, P. Simeoni, and G. Piazza, “33 ghz overmoded bulk acoustic resonator,” *IEEE Microwave and Wireless Components Letters*, vol. 32, no. 6, pp. 656–659, 2022.
- [9] Z. Schaffer, A. Hassani, M. A. Masud, and G. Piazza, “A solidly mounted 55 ghz overmoded bulk acoustic resonator,” in *2023 IEEE International Ultrasonics Symposium (IUS)*. IEEE, 2023, pp. 1–4.
- [10] G. Wingqvist, F. Tasnadi, A. Zukauskaite, J. Birch, H. Arwin, and L. Hultman, “Increased electromechanical coupling in w- scxal1- xn,” *Applied Physics Letters*, vol. 97, no. 11, 2010.
- [11] D. Royer and E. Dieulesaint, “Elastic waves in solids ii,” 2000. [Online]. Available: <https://api.semanticscholar.org/CorpusID:138680523>
- [12] S. Barth, T. Schreiber, S. Cornelius, O. Zyowitzki, T. Modes, and H. Bartzsch, “High rate deposition of piezoelectric alscn films by reactive magnetron sputtering from alsc alloy targets on large area,” *Micromachines*, vol. 13, no. 10, p. 1561, 2022.
- [13] J. D. Larson, P. D. Bradley, S. A. Wartenberg, and R. C. Ruby, “Modified butterworth-van dyke circuit for fbar resonators and automated measurement system,” *2000 IEEE Ultrasonics Symposium. Proceedings. An International Symposium (Cat. No.00CH37121)*, vol. 1, pp. 863–868 vol.1, 2000. [Online]. Available: <https://api.semanticscholar.org/CorpusID:122447790>
- [14] S. Cho, O. Barrera, P. Simeoni, E. N. Marshall, J. Kramer, K. Motoki, T.-H. Hsu, V. Chulukhadze, M. Rinaldi, W. A. Doolittle, and R. Lu, “Millimeter wave thin-film bulk acoustic resonator in sputtered scandium aluminum nitride,” *Journal of Microelectromechanical Systems*, vol. 32, no. 6, pp. 529–532, 2023.